Radar arc and impairment detection and localization for the ITER ICRF antenna

Simone Porporato[1*], *Riccardo* Maggiora[1], *Daniele* Milanesio[1], *Sara* Salvador[1], *Walid* Helou[2], and *Kenji* Saito[2]

[1] Politecnico di Torino, Corso Duca degli Abruzzi 24, 10129 Torino, Italy
[2] ITER Organization, Route de Vinon-sur-Verdon, CS 90 046, 13067 St. Paul Lez Durance Cedex, France

Abstract. A RAdar Arc and impairments Detection and localization (RAAD) system for the protection of high-power RF transmission lines components is presented. It offers several benefits over existing techniques. It can perform fast detection, localization, and classification of arcs and impairments/degradations along the full path of the RF power (in less than 5 µs as required for the protection of ITER ICRF antenna). It also features completely independent operations from the RF power. The detection and monitoring of impairments/degradations enables the prevention of faults while the localization and classification of faults permits pinpoint maintenance operations. The RAAD system has been simulated in time domain adopting the Simulink tool, integrated into the complete ITER ICRF system (from the array antenna front-face up to the RF sources outputs, including the full transmission line and matching network). The radar signal is coupled into the transmission lines through a specifically designed coupling unit. Full wave simulations of the ITER ICRF system components have been performed in the radar bandwidth of operation, with and without arcs/impairments, to obtain S-matrices used in the time domain radar system simulations. All the arcs and impairments inserted in the components have been detected; the location obtained by the radar for each event has been compared to the one estimated analytically with excellent agreement. The radar simulations have demonstrated the ability to detect and localize arcs which cannot be detected by other systems such as low voltage arcs and series arcs. A solid solution, based on signal synchronization, for coping with high power interferences from ion cyclotron frequency harmonics in the radar bandwidth of operations has been implemented. Other events such as antenna load variations and matching elements modifications can be easily discriminated against arc events, being much slower than radar pulse repetition period. Next steps will be the implementation, testing and validation of a prototype of the complete RAAD system. This prototype will be tested on the ITER ICRF prototype antenna module and potentially on other operating ICRF installations.

1 Introduction

The ITER ICRF antenna and transmission line system must be continuously monitored by redundant fast arc detection systems that are based on different concepts. The RAdar Arc Detection (RAAD) is one of the potential candidates. It offers not only the detection of arcs but also their localization and classification. Moreover, it allows the detection and localization of impairments, which is unique to the RAAD system and allows to take different actions depending on the location of the faults. It was already proposed [1] and tested with a low performance and low cost version in the past [2][3]. The unavailability of budget stopped further system development. On the contrary, a system for the adoption in high power transmission lines system used for TV and radio broadcasting has been developed. The system has become a patented product (US20240369610A1) and is currently commercialized and already installed in hundreds of locations proving its usefulness.

This work developed under a contract with the ITER Organization is a numerical investigation to determine the applicability of the RAAD to the complete ICRF system of ITER.

* Corresponding author: simone.porporato@polito.it

2 The RAAD system

The RAAD system is an active arc detection method, it transmits a specific digitally modulated signal along the transmission line and simultaneously it records and processes the echoes (see Fig. 1). The processing, after the down conversion, is based on the correlation of the received signal with the transmitted one. This pulse compression process is what gives the RAAD the ability to accurately locate the arcs. For further details on pulse compression, the reader is referred to [4]. To determine the presence of the arcs and impairments the pulse compressed signal is compared to a combination of previous pulses called background which does not contain arcs.

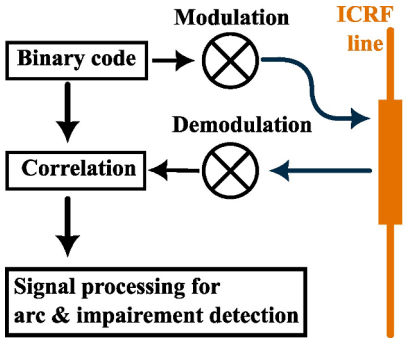

Fig 1. RAAD processing block diagram.

© The Authors, published by EDP Sciences. This is an open access article distributed under the terms of the Creative Commons Attribution License 4.0 (https://creativecommons.org/licenses/by/4.0/).

2.1 System description

The RAAD system, illustrated in Fig. 2, consists of the following hardware: an FPGA to perform all the real time digital processing and waveform generation, a Digital to Analog Converter (DAC) to generate the transmitted waveform, a power amplifier (PA) to increase the transmitted (Tx) signal power up to 100 W, a proper Coupling Unit (CU) to transmit and receive the radar signal along the transmission line, a band pass filter to select the frequency range of the radar signal in reception, and a fast Analog to Digital Converter (ADC) to capture the signal for the processing. The RAAD also needs a reference signal to synchronize with the ICRF frequency, which can be provided by the plant (preferred) or can be derived from the received signal with few additional components.

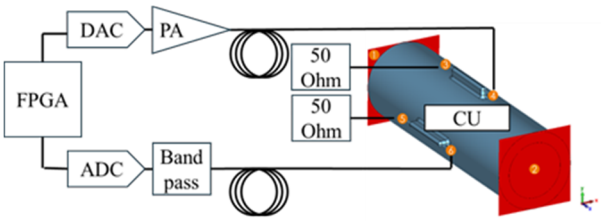

Fig. 2. RAAD system hardware block diagram.

2.2 Radar system parameters

The radar transmitted signal is generated completely in the digital domain, allowing great system flexibility. It is a phase modulated continuous wave signal. A sinusoidal carrier is modulated with a specific binary sequence; in this case, Golay complementary binary sequences are used. The carrier frequency is in the range of 190-240 MHz; the actual value depends on the ICRF frequency synchronization for harmonics suppression. The null-to-null bandwidth of the signal is equal to half of the carrier frequency; this is an important parameter as it determines the radar resolution (the ability to separate two close events in range). The carrier frequency is selected to obtain the largest bandwidth while remaining below the coaxial higher order mode cut-off frequency.

The sequences are transmitted periodically; their starting point is timed according to a Pulse Repetition Interval (PRI). This parameter controls the responsiveness of the system, as the output will be update with a frequency equal to the inverse of the PRI. The length of the sequence will be either 64 or 128 bits depending on the PRI; longer sequences are more resilient to noise and interference but reduce the responsiveness.

On the receiving side the characteristics of the ADC are very important; the accuracy of the localization depends on the sampling frequency ($\Delta x = c/f_s$), while the number of bits controls the dynamic range.

2.3 Custom coupling unit

To transmit and receive the radar signal to and from the transmission line system a dedicated coupling unit is needed. Past experiments [3] employed a single septate coupler with a circulator to separate the transmission and reception path.

ITER design guidelines require no protruding structures inside the coaxial line, electric field below 2 kV/mm with 45 kV on the transmission line and the compatibility with shot duration of 3600 s. These limitations rule out the use of the septate coupler or loop couplers available from industry.

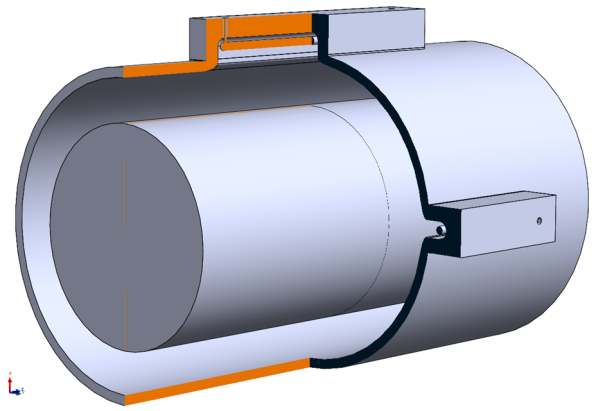

Fig. 3. DCU 3D model.

A custom DCU (Double Coupling Unit), shown in Fig. 3, has been designed to meet the ITER ICRF design guidelines. The DCU contains two identical directional couplers, one used for transmission, and one used for reception. Two separate coupling straps are needed because circulators do not provide sufficient isolation and have a limited fractional bandwidth in the frequency of RAAD operation.

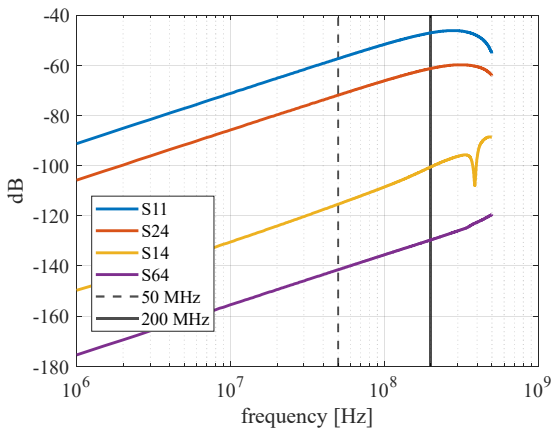

Fig. 4. DCU S-parameters, simulated in CST.

In Fig. 4 the relevant scattering parameters of the coupler are presented; ports 1 and 2 are on the main transmission 12'' coaxial line; ports 3 and 4 are on the Tx coupling strap; ports 5 and 6 are on the Rx coupling strap. The coupling at the RAAD operating frequency is -60 dB; it has been necessary to reduce the coupling due to thermal limitation on the coupling strap; in other system the coupling can be easily increased by changing the strap depth with respect to the coaxial line outer conductor. The coupler has a directivity larger than 35 dB and the direct coupling between Tx and Rx is lower than -120 dB.

3 RAAD time domain simulation

To perform simulation of the RAAD operations in a complex transmission line system in time domain Simulink simulation tool has been adopted. Models have been created accurately representing the desired transmission line system. All the signals needed as inputs (ion cyclotron signal, radar signal, etc.) have been generated with a preprocessing script in MATLAB. The signal captured by the coupling units, which is the result of the simulations, is saved to perform the radar processing in a separate script using MATLAB.

Two classes of Simulink models have been developed: one made of closed form components, which has been used to test the RAAD system during transient and to evaluate the effects of interferers, and a second one, containing components modelled by scattering matrices, used to test the detectability of arcs and impairments inserted in a more realistic transmission line system model.

3.1 Closed form components model

The RAAD system has been initially simulated in a transmission line circuit which represents a single line of the complete ITER ICRF system; all the components except the DCU are modelled in closed form. The antenna load has been modelled with a resistor which has the possibility of being varied during the simulation to simulate loading variations. The arc has been modelled with an inductor with a time varying inductance. When the arc is in the OFF state the inductance is set to 10^{20} H; when the arc switches to the ON state the inductance is set to 100 nH which is a conservative value compared to the 30 nH used in [5]. The transition between the OFF state and the ON state is not instantaneous but follows a sigmoid curve with a rise time that can be set arbitrarily; all the results presented here have been obtained with a rise time equal to 1 ns.

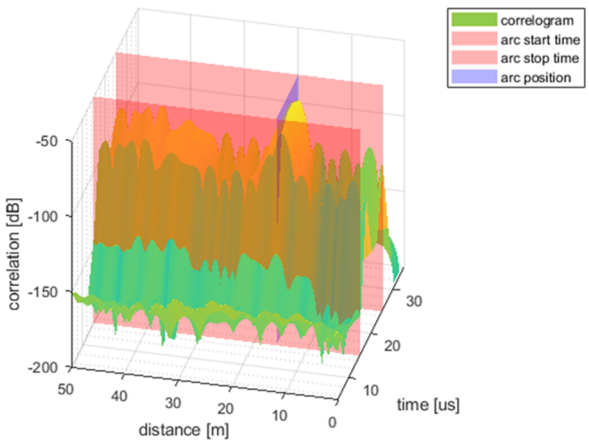

Fig. 5. Correlogram during arcing even and subsequent switch off.

During a simulation run the RAAD signal is continuously and periodically transmitted; at a certain time point the arc is switched from the OFF state to the ON state and after few µs the arc gets turned off again.

In Fig. 5 an example of correlogram is presented. This is the visual output of the RAAD received signal in which the moment when the arc turns on and off is clearly visible, and, at the same time, the distance of the arc from the DCU can be easily determined.

3.1.1 Effect of system variations and plasma emissions

Plasma loading variations are expected to be slow with respect to the PRI and, for this reason, they can be discriminated from arcing events as they are integrated in the background creation algorithm. Moreover, the effects of plasma loading variation are limited to the position outside of the antenna, which allows further discrimination.

In the ITER ICRF system, the matching system variations do not influence the RAAD system operations because all the tuning components are not in the section of line being monitored. The RAAD can also be used to monitor the matching section of an ICRF system, the responsiveness and accuracy will remain the same. The movements of the tuning components that are in the section of line being monitored by the RAAD will not interfere with the radar functionality as they are slow compared to the PRI. The presence of the stubs and decouplers will generate ambiguities as there might be multiple location associated with a given distance from the DCU. There might be possible disambiguation procedures but these need further studies. Moreover the decouplers might cause some coupling between the different radar units (one installed on each line) that can solved by using complementary sequences.

The RAAD, thanks to its phase modulated waveform, is extremely resilient to noise and external interferers. The effect of plasma emissions will be observed and assessed during the future experimental campaign at ASDEX upgrade, with the intention of making plasma scenarios rich of emissions.

3.1.2 Effects of ICRF harmonics

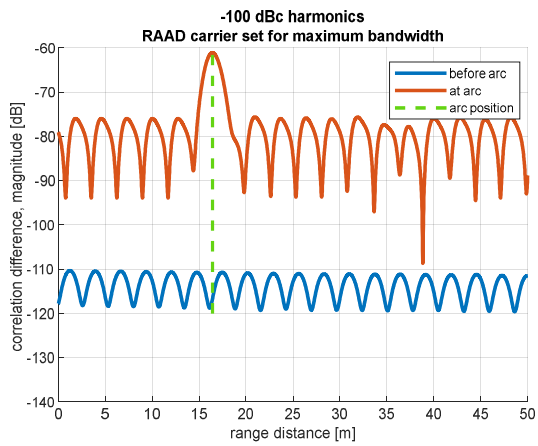

Fig. 6. RAAD response without proper synchronization to the ICRF.

The ICRF harmonics are known interferers that may fall inside the radar bandwidth and can have higher power compared to the radar received signal. In the initial

simulations, low power harmonics caused a ripple in the RAAD response. As the power of the harmonics increases the radar functionality could be compromised.

A solution, based on signal synchronization, has been developed that eliminates the undesired effects of harmonics. Two conditions on the radar signal timing must be respected. First the radar carrier must be an integer multiple of the ICRF frequency, second the PRI must be selected according to (1).

$$PRI = n\frac{1}{2f_{ICRF}} \quad \{n = 2k + 1 \,|k \in \mathbb{N}\}. \qquad (1)$$

With these parameters selection, after the down conversion of the received signal, the ICRF and its harmonics retains the 180° phase shift such that the harmonics from subsequent pulses cancel each other.

In Fig. 6 the ripple on the radar response due to the harmonic's interference is clearly visible: the ICRF power has been set to 1 MW and the radar power to 1 W; all harmonics up to the 6th one were set to -100 dBc.

In Fig. 7 the radar response of the system in the same condition of Fig. 6 but with proper synchronization is presented and the ripple is totally eliminated.

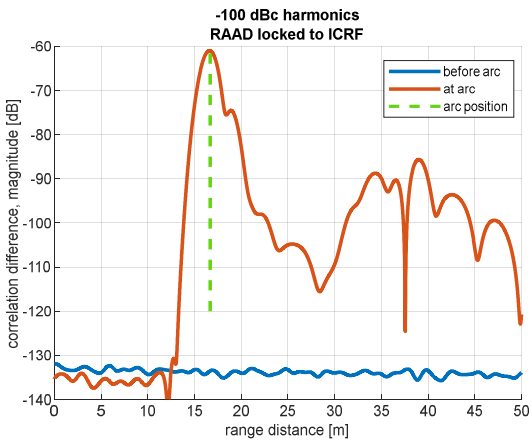

Fig. 7. RAAD response with proper synchronization to the ICRF.

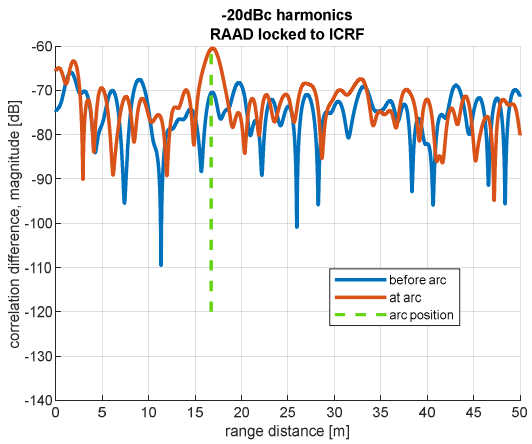

Fig. 8. RAAD response with synchronization and extremely high harmonics level.

In Fig. 8 the level of all harmonics up to the 6th one has been increased to an unrealistic level of -20 dBc, still the arc can be detected and localized. It can be noticed that the traces are much noisier than in the previous cases, this is because most of the ADC dynamics is allocated to the harmonics instead of the radar signal.

3.2 Full wave components model

To test the effectiveness of the RAAD for the ICRF system of ITER, full wave simulations (up to 350 MHz) of the ITER antenna and TL components have been performed. We refer the interested reader to [6] for a detailed description of the methodology. For each component, without arcs and with arcs in different position a scattering matrix has been generated to be inserted into the Simulink simulations in place of the previously closed form modelled components.

It is not possible to switch the arc ON and OFF inside a scattering matrix block in a single simulation. For this reason, a first simulation has been run without arcs to compute the background and then a simulation for each arcing condition has been run. For all simulations all the inputs have been kept equal and just the scattering matrix blocks have been changed. The processing for all arcs and impairments has been done by using the same background.

3.2.1 Arcs on a single ITER ICRF line

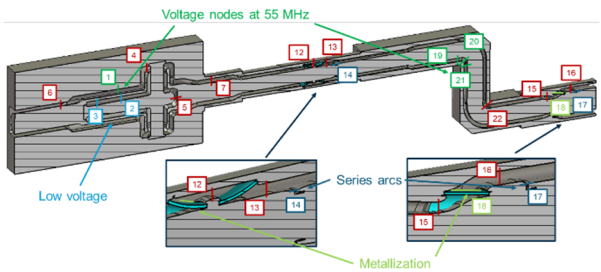

Fig. 9. Arcs inserted in the ITER transmission line to test the RAAD detection.

Many arcs and impairments have been simulated and they are shown in Fig. 9. Among all the arcs in generic positions, there are arcs in low voltage regions, arcs in voltage nodes of the ICRF, ceramics metallization and series arcs occurring in the central conductor joints.

In Fig. 10 an example of the RAAD response is presented where each curve shows a peak in the location of the arc. It must be noted that for the following plots the processing has been performed considering a realistic quantization from the ADC.

The arcs distances from the DCU obtained with the RAAD processing have been compared to the one estimated analytically. There is very good agreement between the two, as it can be observed in Table 1. The distance detected for Arc 5 shows a large difference with respect to the estimated one, instead of a single peak at the expected distance there are two peaks, this is caused by the arc location which is in the symmetry plane of the transmission line. It must be considered that the information of the time domain signal from the full wave simulations has been compressed into a scattering matrix, which has been fitted to allow transformation into the time domain for simulations. Along this process some information can be lost, explaining the not perfect but still very good match.

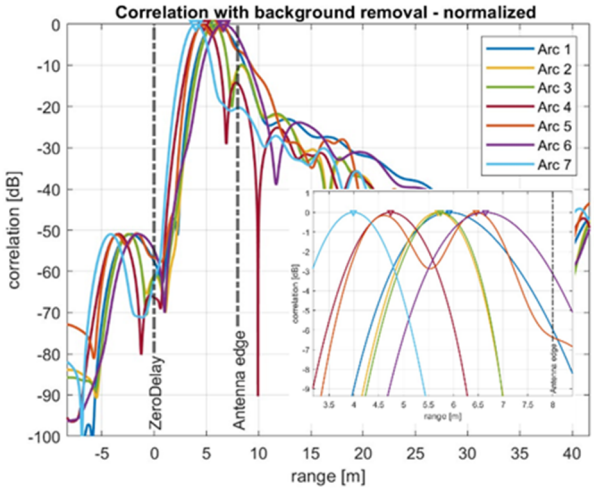

Fig. 10. Example of RAAD response from different arcs in the ITER service stub.

Table 1. Comparison of arc distance estimated by the RAAD and analytically.

Arc location	RAAD [m]	Analytical [m]
Flexible Junction Arc A	0.73	0.763
Rear Window Arc 15	1.30	1.283
Rear Window Arc 16	1.18	1.112
Rear Window Arc 17	1.21	1.022
Rear Window Arc 18 (Impairment)	1.24	1.155 – 1.270
ATLIS Arc 19	2.40	2.365
ATLIS Arc 20	2.25	2.225
ATLIS Arc 21	2.10	2.085
ATLIS Arc 22	1.67	1.606
Front Window Arc 12	3.65	3.392
Front Window Arc 13	3.32	3.236
Front Window Arc 14	3.36	3.155
Fron Window Impairment	3.73	3.445 – 3.513
VTL1-STS-VTL2 Arc 7	3.99	3.971
VTL1-STS-VTL2 Arc 2	5.69	5.770
VTL1-STS-VTL2 Arc 3	5.74	5.927
VTL1-STS-VTL2 Arc 4	4.74	5.164
VTL1-STS-VTL2 Arc 5	6.46	5.564
VTL1-STS-VTL2 Arc 1	5.91	5.933
VTL1-STS-VTL2 Arc 6	6.65	6.415
Arc B (Antenna)	6.61	6.910
Arc E (Antenna)	7.86	7.107
Arc D (Antenna)	7.35	7.437

3.2.2 Arcs on the complete ITER ICRF system

The single line circuit has been expanded to model the complete ICRF system made of eight lines. In this case one RAAD system is installed for each line to also evaluate the cross coupling between the different RAAD units.

In Fig. 11 it can be observed that when an arc occurs in the antenna it gets detected by all RAAD systems with the strongest effect from the line on which the arc has occurred. When an arc occurs inside the transmission lines, as shown in Fig. 12, it is detected only by the RAAD module of the line on which the arc happened (line 1 in the proposed example). This proves that the RAAD modules can operate independently without interfering with each other.

Fig. 11. RAAD response from all line for an arc occurring in the antenna

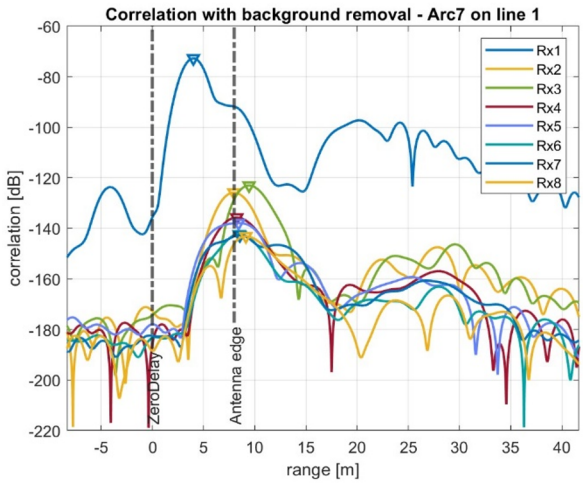

Fig. 12. RAAD response from all lines for an arc occurring inside one of them (line 1).

4 Conclusion and future work

Time domain simulations demonstrated that the RAAD system is capable of detecting arcs and impairments in all locations correctly, both inside different components of the ITER circuits and inside the antenna. Twenty-three different arc's locations have been simulated: all arcs manifest as a high peak in the correlation signals, and they can be correctly localized with high accuracy.

The RAAD system is able to discriminate arcs from matching system variations and load variations. A solution to deal with ICRF harmonics has been developed. The effect of plasma emissions will be assessed during the future experimental campaign.

Next steps include the assembly of a RAAD system prototype and the software and firmware development.

Subsequent installation and testing have been planned to take place in ASDEX upgrade during plasma operation to evaluate the performance in a real environment. There is specific interest to evaluate the effects of Ion Cyclotron Emissions and of Edge Localized Modes.

Finally, the RAAD system will be tested on the ITER prototype antenna module during vacuum

operation to evaluate its functionality on the target system.

This work has been conducted under contract IO/24/CT/4300003010. The views and opinions expressed herein do not necessarily reflect those of the ITER Organization.

References

1. R. Maggiora, S. Salvador; UWB radar technique for arc detection in coaxial cables and waveguides, AIP Conf. Proc. **1187**, 261–264 (2009). https://doi.org/10.1063/1.3273743
2. S. M. Salvador, R. Maggiora, R. D'Inca, H. Fuenfgelder; Arc Detection With GUIDAR: First Experimental Tests On MXP Testbed, AIP Conf. Proc. **1406**, 25–28 (2011). https://doi.org/10.1063/1.3664921
3. S. M. Salvador, R. Maggiora, R. H. Goulding, J. A. Moore, R. I. Pinsker, A. Nagy; Guided radar system for arc detection: Initial results at DIIID. AIP Conf. Proc. **1580**, 283–286 (2014). https://doi.org/10.1063/1.4864543
4. M. I. Skolnik, Radar handbook, third edition (McGraw-Hill, New York, 2008)
5. Monakhov, V. Bobkov, M. Graham, M.-L. Mayoral, K. Nicholls, A. Walden, JET EFDA contributors, Voltage Node Arcing in the ICRH Antenna Vacuum Transmission Lines at JET, AIP Conf. Proc. **933**, 151–154 (2007). https://doi.org/10.1063/1.2800464
6. D. Milanesio et al., Full-wave modeling of arcs within the ITER ICRF antenna for usage in the simulations and design of the RADAR Arc Detection system, 25th Topical Conference on Radio-Frequency Power in Plasmas, Schloss Hohenkammer, Germany, May 19-22 (2025)